Surface diffusion on a stepped surface

Akiko Natori* and Rex W. Godby
Cavendish Laboratory, University of Cambridge, Madingley Road, Cambridge CB3 0HE, United Kingdom
(Received 10 September 1992)

Surface diffusion of an adatom on a vicinal surface is investigated, using site-dependent hopping rates based on a model surface-potential profile of a regularly stepped surface. We solved analytically the coupled rate equations for the occupation probability of an adatom at a sufficiently long time, in analogy to the tight-binding theory of electronic structure. From this, the general relation between the hopping rates and the diffusion coefficient is derived. Formulas of both surface diffusion coefficients, parallel and perpendicular to a step edge direction, are obtained as functions of related atomic hopping rates at a terrace site, an upper edge site, and a lower edge site and of the step spacing. The fundamental mechanism determining the crucial role of step arrays on surface diffusion is clarified. No difference was found between step-up diffusion and step-down diffusion, even in the absence of inversion symmetry on the surface-potential profile. With Monte Carlo simulation, the effect of kink sites on surface diffusion is studied. Kinks greatly suppress the parallel diffusion coefficient, while they suppress only weakly the perpendicular diffusion coefficient.

I. INTRODUCTION

Surface diffusion is the most fundamental process of mass transport on the solid surface, and it plays a crucial role in crystal growth, catalysis, and corrosion. Recently vicinal surfaces have attracted interest both for the fundamental surface physics and for their applications to crystal growth.[1,2] Surface diffusion on a stepped surface was investigated by Roulet[3] for the first time. Since then several experimental studies have been performed. In some cases, strong enhancement of diffusion was observed in the direction of a step edge,[4–6] sometimes accompanied by suppression in the direction perpendicular to a step edge.[6] With respect to the difference between step-up diffusion and step-down diffusion, two contradictory results were reported, one detecting a difference[7] and the other failing to do so.[6] Recently the surface-potential profile for an adatom on a vicinal surface was calculated for metal,[8–10] using empirical many-body interatomic potentials. On the flat semiconductor surface, the first-principles pseudopotential method was also applied[11] to the calculation of the surface-potential profile. The calculated potential profile depends strongly on both the material and the index of a vicinal surface. However, three common features emerge. (i) The binding energy of an adatom at a lower edge site of a step is larger than that on a terrace, i.e., a lower edge site acts as a trap center for adatoms on a terrace. (ii) The diffusion activation energy is lower along a lower step edge than on a terrace. (iii) The binding energy of an adatom at a kink site is larger than that at a lower edge site, i.e., a kink site acts as a trap center for adatoms diffusing along a lower step edge. Recently molecular-dynamics calculation has been applied[10] to a vicinal surface with short step spacings. In molecular dynamics the hopping rates at specific sites can be obtained directly, although the size of system is very limited.

The purpose of this paper is to investigate the surface diffusion of an adatom in both directions, parallel and perpendicular to a step edge. We start from the coupled rate equations for the adatom occupation probabilities, using site-dependent hopping rates based on a model surface-potential profile.[12] From the long-time behavior of this solution, we derive the general relation between the diffusion coefficient and the hopping rates. With use of this relation, the analytical formula of the surface diffusion coefficient is obtained in the case of a regularly stepped surface. The effect of kink sites is also studied by means of Monte Carlo simulation.

II. SURFACE DIFFUSION ON A REGULARLY STEPPED SURFACE

In this section we calculate the tracer diffusion coefficient of an adatom on a regularly stepped surface, based on a simple lattice-gas model[12] with a square lattice. We assume for an adatom the simple potential profile characterizing a regularly stepped surface as shown in Fig. 1. Corresponding to this potential profile, five kinds of characteristic hopping rates to the nearest-neighbor sites are defined: Γ, the hopping rate from a terrace site to its nearest-neighbor sites, and that from an upper edge site to the nearest upper edge or terrace sites; Γ_1 from a lower edge site to a terrace site; Γ_2 along a lower step edge; ΓS from an upper edge site to a lower edge site; and $\Gamma_1 S$ from a lower edge site to an upper edge site. Here S is the so-called Schwoebel factor,[13,14] and it is related to the extra energy barrier E_S (see Fig. 1) at a step edge.

$$S = \exp(-E_S/kT) , \tag{1}$$

where k is the Boltzmann constant and T the temperature. The surface potential of a regularly stepped surface has a periodicity due to the step structure. Its unit cell

has an area of $a \times na$, indicated by a hatched region in Fig. 1. a is a lattice constant of a square lattice and na is a step spacing. We consider the tracer diffusion coefficient[15] in the limit of a low adatom density, so that both the exclusion principle and the interaction among adatoms can be neglected. In this limit the tracer diffusion coefficient becomes equal to the chemical diffusion coefficient,[15] and it is the most fundamental quantity of surface diffusion.

The rate equations of the occupation probability $P_j(l,m,t)$ at the jth site in the unit cell indexed by (l,m) are written as follows:

$$\begin{aligned}
\frac{d}{dt}P_1(l,m,t) &= -(2\Gamma_2+\Gamma_1+\Gamma_1 S)P_1(l,m,t)+\Gamma P_2(l,m,t)+\Gamma S P_n(l-1,m,t)+\Gamma_2[P_1(l,m+1,t)+P_1(l,m-1,t)] , \\
\frac{d}{dt}P_2(l,m,t) &= -4\Gamma P_2(l,m,t)+\Gamma P_3(l,m,t)+\Gamma_1 P_1(l,m,t)+\Gamma[P_2(l,m+1,t)+P_2(l,m-1,t)] , \\
\frac{d}{dt}P_j(l,m,t) &= -4\Gamma P_j(l,m,t)+\Gamma[P_{j+1}(l,m,t)+P_{j-1}(l,m,t)]+\Gamma[P_j(l,m+1,t)+P_j(l,m-1,t)] , \\
\frac{d}{dt}P_n(l,m,t) &= -(3\Gamma+\Gamma S)P_n(l,m,t)+\Gamma_1 S P_1(l+1,m,t)+\Gamma P_{n-1}(l,m,t)+\Gamma[P_n(l,m+1,t)+P_n(l,m-1,t)] .
\end{aligned} \tag{2}$$

For each site in a unit cell from a lower edge site to an upper edge site (see Fig. 1), j is numbered from 1 to n. It should be noticed that the total sum of $P_j(l,m,t)$ with j, l, and m is conserved. These coupled linear equations have a similar form to those in the tight-binding theory of electronic structure, if t is replaced by $t/i\hbar$ and if hopping rates are replaced by the corresponding Hamiltonian matrix elements. So we can solve Eq. (2) using the analogy with tight-binding theory. At first we calculate eigenvalues, and then expand $P_j(l,m,t)$ with eigenfunctions, and finally calculate the long-time behavior of $P_j(l,m,t)$ by determining the expansion coefficients from an appropriate initial condition at $t=0$. This is the opposite of the quantum Monte Carlo method[16] in which the ground state is obtained as the asymptotic solution at a sufficiently long time of the corresponding diffusion equation derived from the Schrödinger equation in imaginary time.

The eigenvalues can be calculated with use of the Fourier transform of $P_j(l,m,t)$.

$$p_j(k_x,k_y,t)=\frac{1}{\sqrt{N_x N_y}}\sum_{l=1}^{N_x}\sum_{m=1}^{N_y} e^{-ik_x a(nl+j)} e^{-ik_y am} \times P_j(l,m,t) , \tag{3}$$

where N_x and N_y are the number of unit cells in x and y directions, respectively. The rate equations for $p_j(k_x,k_y,t)$ can be written as

$$\begin{aligned}
\frac{d}{dt}p_1(k_x,k_y,t) &= [-(2\Gamma_2+\Gamma_1+\Gamma_1 S)+2\Gamma_2\cos(k_y a)]p_1(k_x,k_y,t)+\Gamma e^{ik_x a}p_2(k_x,k_y,t)+\Gamma S e^{-ik_x a}P_n(k_x,k_y,t) , \\
\frac{d}{dt}p_2(k_x,k_y,t) &= \Gamma_1 e^{-ik_x a}p_1(k_x,k_y,t)+[-4\Gamma+2\Gamma\cos(k_y a)]p_2(k_x,k_y,t)+\Gamma e^{ik_x a}p_3(k_x,k_y,t) , \\
\frac{d}{dt}p_j(k_x,k_y,t) &= \Gamma e^{-ik_x a}p_{j-1}(k_x,k_y,t)+[-4\Gamma+2\Gamma\cos(k_y a)]p_j(k_x,k_y,t)+\Gamma e^{ik_x a}p_{j+1}(k_x,k_y,t) , \\
\frac{d}{dt}p_n(k_x,k_y,t) &= \Gamma_1 S e^{ik_x a}p_1(k_x,k_y,t)+\Gamma e^{-ik_x a}p_{n-1}(k_x,k_y,t)+[-(3\Gamma+\Gamma S)+2\Gamma\cos(k_y a)]p_n(k_x,k_y,t) .
\end{aligned} \tag{4}$$

The $n \times n$ matrix constituted by coefficients on $p_j(k_x,k_y,t)$ on the right-hand side has three nonzero elements in each row, and is defined as H hereafter. The n eigenvalues $\omega_\lambda(\mathbf{k})$ $(\lambda=1,2,\ldots,n)$ of H are the solutions of the following secular equation:

$$\det(H-\epsilon I)\equiv g(\mathbf{k},\epsilon)=0 , \tag{5}$$

where $I_{i,j}=\delta_{i,j}$. With use of these eigenvalues $\omega_\lambda(\mathbf{k})$, $p_j(\mathbf{k},t)$ can generally be written as

$$p_j(\mathbf{k},t)=\sum_{\lambda=1}^{n} c_{j\lambda}(\mathbf{k})e^{\omega_\lambda(\mathbf{k})t} . \tag{6}$$

With respect to the initial condition at time $t=0$, the following condition is imposed:

$$P_j(l,m,0)=0 \quad \text{for} \quad (l,m)\neq(0,0) . \tag{7}$$

Then $p_j(\mathbf{k},0)$ can be written as

$$p_j(\mathbf{k},0)=\frac{1}{\sqrt{N_xN_y}}P_j(\mathbf{0},0)e^{-ik_xaj} . \tag{8}$$

This initial condition can be satisfied, provided

$$c_{j\lambda}(\mathbf{k})\propto e^{-ik_xaj} . \tag{9}$$

We are interested in the long-time behavior, and only the highest energy branch $\lambda=1$ is dominant in this limit. It is proved later that there exists an energy branch with the following dispersion relation:

$$\omega_1(\mathbf{k})=-a_xk_x^2-a_yk_y^2 . \tag{10}$$

Positive eigenvalues are forbidden physically, since this brings about the divergence of the probability in the limit of $t\rightarrow\infty$. As mentioned before, the total sum of $P_j(l,m,t)$ is conserved. So, $\omega_1(\mathbf{k})$ just corresponds to the highest energy branch. From Eqs. (6), (9), and (10), the long-time behavior of $P_j(l,m,t)$ can be expressed as

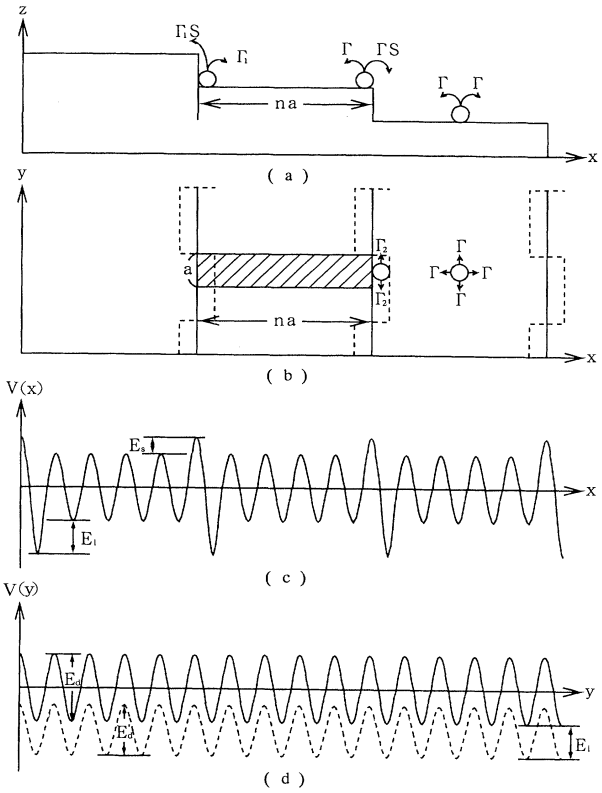

FIG. 1. A section (a) and a plane figure (b) of a regularly stepped surface. The hopping rates of an adatom to the nearest-neighbor sites are shown with arrows. The corresponding potential profile (c) in the x direction and those (d) in the y direction, on terrace sites (solid line) and along lower edge sites (broken line). In (b), a hatched area indicates a unit cell of the surface potential. The broken line in (b) shows a periodic kink structure, assumed in Sec. III.

$$\begin{aligned}P_j(l,m,t)&=\frac{1}{\sqrt{N_xN_y}}\sum_{k_x}\sum_{k_y}p_j(\mathbf{k},t)e^{ik_xa(nl+j)}e^{ik_yam}\\&\sim\frac{1}{\sqrt{N_xN_y}}\frac{anN_x}{2\pi}\frac{aN_y}{2\pi}\int dk_x\int dk_yc_{j1}(\mathbf{k})e^{\omega_1(\mathbf{k})t}e^{ik_xa(nl+j)}e^{ik_yam}\\&\sim\frac{1}{(2\pi)^2}\int dk_xe^{-a_xk_x^2t}e^{ik_xanl}\int dk_ye^{-a_yk_y^2t}e^{ik_yam}\\&=\frac{1}{\sqrt{4\pi a_xt}}\exp[-(anl)^2/4a_xt]\frac{1}{\sqrt{4\pi a_yt}}\exp[-(am)^2/4a_yt] .\end{aligned} \tag{11}$$

On the other hand, the probability function $P(x,y,t)$ for an adatom starting from $(x,y)=(0,0)$ at time $t=0$ is related with its diffusion coefficients D_x and D_y in the x and y directions as

$$P(x,y,t)=\frac{1}{\sqrt{4\pi D_xt}}\exp(-x^2/4D_xt)\frac{1}{\sqrt{4\pi D_yt}}\exp(-y^2/4D_yt) . \tag{12}$$

From the comparison between Eqs. (11) and (12), we conclude that

$$\begin{aligned}D_x&=a_x ,\\D_y&=a_y .\end{aligned} \tag{13}$$

Further, Eq. (11) means the diffusion coefficient in the x direction does not depend on the sign of l, i.e., step-up or step-

down directions.

Now, let us study the eigenvalues of the secular equation. $g(\mathbf{k},\epsilon)$ defined by Eq. (5) can be written explicitly as

$$g(\mathbf{k},\epsilon)=\{[-(2\Gamma_2+\Gamma_1+\Gamma_1 S)+2\Gamma_2\cos(k_y a)-\epsilon][-(3\Gamma+\Gamma S)+2\Gamma\cos(k_y a)-\epsilon]-\Gamma_1\Gamma S^2\}f_{n-2}(\mathbf{k},\epsilon)$$
$$+\{-\Gamma^2[-(2\Gamma_2+\Gamma_1+\Gamma_1 S)+2\Gamma_2\cos(k_y a)-\epsilon]-\Gamma_1\Gamma[-(3\Gamma+\Gamma S)+2\Gamma\cos(k_y a)-\epsilon]\}f_{n-3}(\mathbf{k},\epsilon)$$
$$+\Gamma_1\Gamma^3 f_{n-4}(\mathbf{k},\epsilon)+\Gamma_1 S(-\Gamma)^{n-1}2\cos(nk_x a)\ . \tag{14}$$

Here $f_j(\mathbf{k},\epsilon)$ is defined as the determinant of the following $j\times j$ matrix:

$$f_j(\mathbf{k},\epsilon)=\det\begin{bmatrix} -4\Gamma+2\Gamma\cos(k_y a)-\epsilon & \Gamma e^{ik_x a} & 0 & \cdots & 0 & 0 \\ \Gamma e^{-ik_x a} & -4\Gamma+2\Gamma\cos(k_y a)-\epsilon & \Gamma e^{ik_x a} & \cdots & 0 & 0 \\ \vdots & & & & & \vdots \\ 0 & 0 & 0 & \cdots & \Gamma e^{-ik_x a} & -4\Gamma+2\Gamma\cos(k_y a)-\epsilon \end{bmatrix}\ . \tag{15}$$

$f_j(\mathbf{k},\epsilon)$ can be simply written with use of their eigenvalues $\epsilon_{j\lambda}(\mathbf{k})$ $(\lambda=1,2,\ldots,j)$ as

$$f_j(\mathbf{k},\epsilon)=\prod_{\lambda=1}^{j}[\epsilon_{j\lambda}(\mathbf{k})-\epsilon]\ , \tag{16}$$

where

$$\epsilon_{j\lambda}(\mathbf{k})=2\Gamma\cos\left[\frac{\pi\lambda}{j+1}\right]-4\Gamma+2\Gamma\cos(k_y a)\ . \tag{17}$$

At first let us notice the existence of a solution of $\omega=0$ at $\mathbf{k}=\mathbf{0}$, i.e., $g(\mathbf{0},0)=0$. This equation can be proved using the following relation:

$$\prod_{\lambda=1}^{j}\epsilon_{j\lambda}(\mathbf{0})=(-\Gamma)^j(j+1)\ , \tag{18}$$

which can be derived from the mathematical formula

$$\prod_{\lambda=1}^{j}\sin\left[\frac{\lambda\pi}{j+1}\right]=\frac{j+1}{2^j}\ . \tag{19}$$

Next we will calculate a_x. This can be obtained as the coefficient of a solution of the order of $(k_x)^2$ of Eq. (5) under the condition of $k_y=0$. $g(k_x,0,\epsilon)$ in Eq. (14) can be expanded in ϵ as

$$g(k_x,0,\epsilon)=c_1\epsilon+c_2\epsilon^2+\cdots+c_n\epsilon^n$$
$$+\Gamma_1 S(-\Gamma)^{n-1}2[\cos(nk_x a)-1]\ , \tag{20}$$

since $g(0,0,0)=0$. Therefore the solution of the order of k_x^2 can be simply given by

$$\epsilon=\frac{\Gamma_1 S(-\Gamma)^{n-1}(nak_x)^2}{c_1}\ . \tag{21}$$

Thus a_x is written as

$$a_x=-\frac{\Gamma_1 S(-\Gamma)^{n-1}(na)^2}{c_1}\ . \tag{22}$$

On the other hand, c_1 can be obtained from Eqs. (14) and (20) as

$$c_1=(-\Gamma)^{n-1}\left[-(1+S)\left[1+\frac{\Gamma_1}{\Gamma}\right](n-1)+\Gamma_1(1+2S)(n-1)\sum_{\lambda=1}^{n-2}\frac{1}{\epsilon_{n-2,\lambda}(\mathbf{0})}+\left[1+\frac{\Gamma_1}{\Gamma}\right](n-2)\right.$$
$$\left.-2\Gamma_1(1+S)(n-2)\sum_{\lambda=1}^{n-3}\frac{1}{\epsilon_{n-3,\lambda}(\mathbf{0})}+(n-3)\Gamma_1\sum_{\lambda=1}^{n-4}\frac{1}{\epsilon_{n-4,\lambda}(\mathbf{0})}\right]\ . \tag{23}$$

With use of the mathematical formula

$$\sum_{r=1}^{n/2-1}\csc^2\left[\frac{r\pi}{n}\right]=\frac{n^2-4}{6}\quad\text{for even } n\ , \tag{24}$$

the next relation is derived:

$$\sum_{\lambda=1}^{j}\frac{1}{\epsilon_{j,\lambda}(\mathbf{0})}=-\frac{1}{6\Gamma}[(j+1)^2-1]\ . \tag{25}$$

Finally c_1 can be simply expressed as

$$c_1=-(-\Gamma)^{n-1}[S(n-1)+1]\left[\frac{\Gamma_1}{\Gamma}(n-1)+1\right]\ . \tag{26}$$

Then a_x is obtained as

$$a_x=\frac{\Gamma(an)^2}{\left[n-1+\frac{1}{S}\right]\left[n-1+\frac{\Gamma}{\Gamma_1}\right]}\ . \tag{27}$$

Next we will derive the expression for a_y. In this case we set $k_x=0$, and calculate the solution of Eq. (5) in the order of k_y^2. For that purpose, we define η as

$$\eta=\epsilon+2\Gamma-2\Gamma\cos(k_y a)\ . \tag{28}$$

Then $g(0,k_y,\eta)$ in Eq. (14) can be written as

$$g(0,k_y,\eta)=(\{2(\Gamma-\Gamma_2)[1-\cos(k_y a)]-\Gamma_1(1+S)-\eta\}[-\Gamma(1+S)-\eta]-\Gamma_1\Gamma S^2)f_{n-2}(0,0,\eta)$$
$$+(-\Gamma^2\{2(\Gamma-\Gamma_2)[1-\cos(k_y a)]-\Gamma_1(1+S)-\eta\}-\Gamma_1\Gamma[-\Gamma(1+S)-\eta])f_{n-3}(0,0,\eta)$$
$$+\Gamma_1\Gamma^3 f_{n-4}(0,0,\eta)+2\Gamma_1 S(-\Gamma)^{n-1}\ . \tag{29}$$

$g(0,k_y,\eta)$ can be expanded in η as before,

$$g(0,k_y,\eta)=c_1\eta+c_2\eta^2+\cdots+c_n\eta^n-2(\Gamma-\Gamma_2)[1-\cos(k_y a)][\Gamma(1+S)+\eta]f_{n-2}(0,0,\eta)$$
$$-\Gamma^2 2(\Gamma-\Gamma_2)[1-\cos(k_y a)]f_{n-3}(0,0,\eta)\ . \tag{30}$$

Here the expansion coefficients c_j are the same as those in Eq. (20). Therefore η can be obtained to second order of k_y as

$$\eta=\frac{1}{c_1}\left[(\Gamma-\Gamma_2)\Gamma(1+S)\prod_{\lambda=1}^{n-2}\epsilon_{n-2,\lambda}(\mathbf{0})\right.$$
$$\left.+\Gamma^2(\Gamma-\Gamma_2)\prod_{\lambda=1}^{n-3}\epsilon_{n-3,\lambda}(\mathbf{0})\right](k_y a)^2\ , \tag{31}$$

where c_1 is given by Eq. (26). Finally ϵ can be written to second order in k_y as

$$\epsilon=-\frac{\Gamma(n-1)+\Gamma_2\dfrac{\Gamma}{\Gamma_1}}{n-1+\dfrac{\Gamma}{\Gamma_1}}(ak_y)^2\ . \tag{32}$$

So, a_y is written as

$$a_y=\frac{\Gamma(n-1)+\Gamma_2\Gamma/\Gamma_1}{n-1+\Gamma/\Gamma_1}a^2\ . \tag{33}$$

Thus we can obtain the following formula for the diffusion coefficient D_x and D_y:

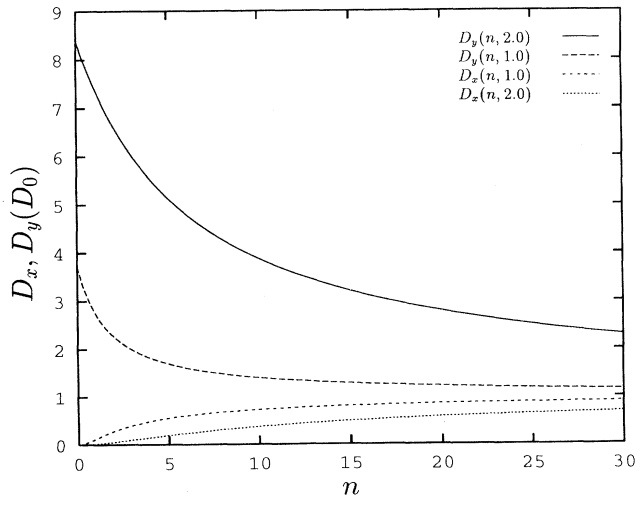

FIG. 2. A parallel diffusion coefficient D_y and a perpendicular diffusion coefficient D_x in a unit of D_0 on a regularly stepped surface as a function of step spacing n. Here the relations of $(E_d-E_d')/kT=E_l/kT=E_S/kT$ are assumed with values of 2.0 (solid line and dotted line) and 1.0 (broken line and short broken line).

$$D_x=\frac{n^2}{\left[n-1+\dfrac{1}{S}\right]\left[n-1+\dfrac{\Gamma}{\Gamma_1}\right]}\Gamma a^2\ ,$$
$$D_y=\frac{n-1+\dfrac{\Gamma}{\Gamma_1}\dfrac{\Gamma_2}{\Gamma}}{n-1+\dfrac{\Gamma}{\Gamma_1}}\Gamma a^2\ . \tag{34}$$

Here Γa^2 is a diffusion constant D_0 of an adatom on a flat surface.

To illustrate these results we take Γ, Γ_1, and Γ_2 as

$$\Gamma=\nu e^{-E_d/kT}\ ,$$
$$\Gamma_1=\nu e^{-(E_d+E_l)/kT}\ , \tag{35}$$
$$\Gamma_2=\nu e^{-E_d'/kT}\ .$$

Here ν is a frequency factor and the same value was assumed for simplicity. Hereafter a is taken as a unit of length and Γ^{-1} is taken as a unit of time. So a diffusion constant D_0 of an adatom on a flat surface becomes unity. D_x and D_y are characterized by four parameters: $(E_d-E_d')/kT$, E_l/kT, E_S/kT, and a step spacing n. D_x and D_y are shown as a function of n in Fig. 2 in the case of $(E_d-E_d')/kT=E_l/kT=E_S/kT$.

III. MONTE CARLO SIMULATION

We have performed Monte Carlo simulations[17] of the surface diffusion of a single adatom to confirm the validity of Eq. (34), and also to study the effect of kink sites. It was neglected in the derivation of Eq. (34), although kinks exist inevitably in steps at finite temperatures.

The time dependence of the mean-square average $\langle x^2\rangle$ and $\langle y^2\rangle$ of the displacement of an adatom was calculated. From Eq. (12), they are related with each diffusion coefficient D_x or D_y as

$$\langle x^2\rangle=2D_x t\ ,$$
$$\langle y^2\rangle=2D_y t\ . \tag{36}$$

The time variation of displacement of an adatom has been simulated with use of the site-dependent hopping rates as indicated in Fig. 1. The ensemble average was taken over 10 000 adatoms. To study the long-time behavior, it is necessary that the displacement be at least

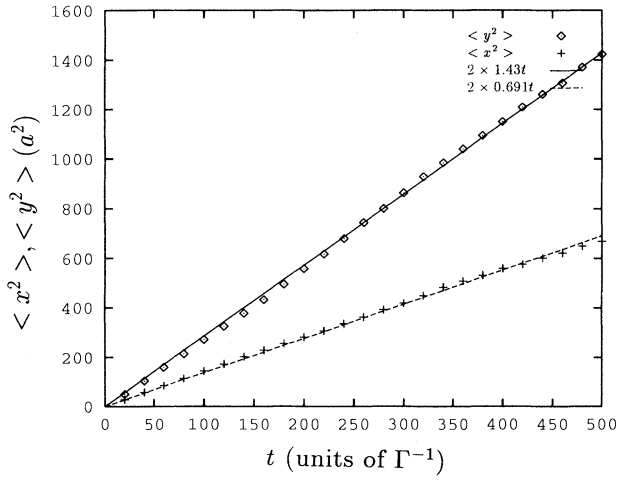

FIG. 3. The mean-square displacements $\langle x^2 \rangle$ and $\langle y^2 \rangle$ in a unit of a^2 as a function of time t in a unit of Γ^{-1} on a regularly stepped surface with $n=10$. Here $(E_d-E_d')/kT=E_l/kT=E_S/kT=1.0$ are taken. The best-fitted relations, $2D_x t$ and $2D_y t$, are drawn by a broken line and a solid line, respectively.

larger than the step spacing. The calculated results of both $\langle x^2 \rangle$ and $\langle y^2 \rangle$ on a regularly stepped surface with $n=10$ are shown in Fig. 3 for the case of $(E_d-E_d')/kT=E_l/kT=E_S/kT=1$. Both $\langle x^2 \rangle$ and $\langle y^2 \rangle$ depend linearly on time t as expected from Eq. (36), and D_x and D_y are obtained as 0.691 and 1.43, respectively. It is remarked that the linear dependence of $\langle x^2 \rangle$ on time means $\langle x \rangle=0$, i.e., the step-up diffusion coefficient is equal to the step-down diffusion coefficient. Theoretical values derived from Eq. (34) are 0.728 and 1.40, and the agreement is satisfactory.

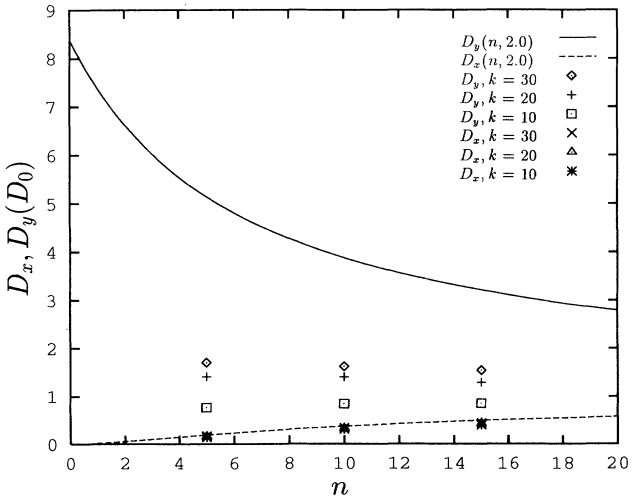

FIG. 4. Parallel diffusion coefficients D_y and perpendicular diffusion coefficients D_x as a function of a step spacing n on a stepped surface with a periodic kink arrangement along each step. Kink intervals $k=30$, 20, and 10 are taken. Here $(E_d-E_d')/kT=E_l/kT=E_S/kT=(E_k-E_l)/kT=2.0$ are assumed. The diffusion coefficients D_y and D_x given by Eq. (34) are shown by a solid line and a broken line, respectively.

Next the effect of kink sites on surface diffusion is studied. We take the kink sites to be arranged periodically along each step as shown schematically by a broken line in Fig. 1(b). An extra binding energy E_k was assumed at a kink site compared to a terrace site. The hopping rates from a kink site to a lower edge site along a step, to an upper edge site and to a terrace site, are therefore taken to be $\Gamma_2 \exp^{-(E_k-E_l)/kT}$, $\Gamma_1 S \exp^{-(E_k-E_l)/kT}$, and $\Gamma_1 \exp^{-(E_k-E_l)/kT}$, respectively. We have calculated both D_x and D_y as functions of a step spacing n, for three values of kink spacings $k=10$, 20, and 30 in a unit of a. We have assumed $(E_d-E_d')/kT=E_S/kT=E_l/kT=(E_k-E_l)/kT=2$. The calculated results are summarized in Fig. 4 with the corresponding functions of Eq. (34). As the kink spacing is decreased, the parallel diffusion coefficient is suppressed remarkably, especially for smaller values of n. On the contrary, a perpendicular diffusion coefficient is only weakly suppressed.

IV. DISCUSSION AND CONCLUSION

Let us discuss the relation with the steady-state solution, to clarify the meaning of each diffusion coefficient given by Eq. (34). Under the steady-state condition, we can solve easily the corresponding diffusion equation. The steady diffusion flux in the y direction can be brought about by fixing the adatom concentrations on a terrace as n_0 at $y=0$ and 0 at $y=L$. Here n_0 and L are appropriate constants to maintain a stationary state. This boundary condition means the adatom concentrations at a lower step edge are $n_0 \exp(E_l/kT)$ at $y=0$ and 0 at $y=L$, since the thermal equilibrium between a lower step edge site and a terrace site at the same y coordinate is maintained in the steady state. The diffusion flux J_{ys} along a lower step edge and J_{yt} on a terrace is simply given as

$$J_{ys}=\Gamma_2 a^2 n_0 e^{E_l/kT}/L \ , \qquad J_{yt}=\Gamma a^2 n_0/L \ . \tag{37}$$

Thus the mean flux $\langle J_y \rangle$ can be written as

$$\langle J_y \rangle = \frac{n_0}{L}\Gamma a^2 \left[\frac{1}{n}\frac{\Gamma_2}{\Gamma}\exp(E_l/kT)+\frac{n-1}{n} \right] . \tag{38}$$

We define the "steady" diffusion coefficient D_{sy} by

$$\langle J_y \rangle = D_{sy}\frac{n_0}{L}\left[\frac{1}{n}e^{E_l/kT}+\frac{n-1}{n} \right] , \tag{39}$$

since the coefficient of D_{sy} is just the average concentration gradient. Then D_{sy} is reduced to the same expression as Eq. (34),

$$D_{sy}=\frac{\frac{\Gamma_2}{\Gamma}e^{E_l/kT}+n-1}{e^{E_l/kT}+n-1}D_0 \ . \tag{40}$$

The above equation means each diffusion path along a lower step edge and on a terrace has a weight of $\exp(E_l/kT)/[\exp(E_l/kT)+n-1]$ and $(n-1)/\exp[(E_l/kT)+n-1]$, respectively. This situa-

tion is also maintained in nonsteady situation, and so D_{sy} is equal to D_y. The increase of a parallel diffusion coefficient compared to D_0 is caused only if Γ_2/Γ is larger than unity. This effect is enhanced by the increase of E_l/kT or by the decrease of n. The existence of kink sites interrupts efficiently the diffusion path along a lower step edge, as seen in Fig. 4.

On the other hand, the steady diffusion flux in the x direction is realized if the adatom concentrations are fixed at two x coordinates. The steady state means the concentration gradient on a terrace has a constant value c independent of time and a coordinate. From the condition of the continuity of a flux at a step edge, the difference δ between the concentrations at two sites on both sides of a lower edge site can be written as

$$\delta=\left[\frac{1}{\Gamma}+\frac{1}{\Gamma S}\right]\frac{Dc}{a} . \tag{41}$$

The "steady" diffusion coefficient D_{sx} is defined by the next relation:

$$J_x=D_{sx}[c(n-2)a+\delta]/na , \tag{42}$$

since the coefficient of D_{sx} is just the average concentration gradient. From the relation of $J_x=D_0c$, D_{sx} can be obtained as

$$D_{sx}=\frac{n}{n-1+\frac{1}{S}}D_0 . \tag{43}$$

Equation (43) means the inverse of D_{sx} is given by the weighted summation of D_0^{-1} with a weight of $(n-1)/n$ and $(D_0S)^{-1}$ with that of $1/n$, as expected from the serial connection of diffusion paths with D_0 and D_0S. This steady-state solution does not depend on Γ_1, and cannot reproduce the previous formula in Eq. (34). In the steady state, the continuity of flux determines the concentration at a lower step edge site, and the effect of E_l is canceled. Contrary to the steady-state solution, the perpendicular diffusion coefficient in Eq. (34) is suppressed by two effects at a step edge, the Schwoebel effect S and the binding effect of an adatom at a lower step edge. Both these effects are strengthened as the step spacing decreases, as seen in Fig. 2. However, the interruption effect at kinks is not so effective as on parallel diffusion as seen in Fig. 4, since there remain much easier diffusion paths across a step edge.

In conclusion, we have succeeded in obtaining the exact analytical formula of both surface diffusion coefficients D_y parallel to a step edge and D_x perpendicular to a step edge, based on a simple potential profile characterizing a regularly stepped surface. No difference was found between the perpendicular diffusion coefficients in the step-up direction and step-down direction even in the presence of the Schwoebel effect S, i.e., without inversion symmetry of the potential profile between the step-up direction and the step-down direction. This is because the product of the hopping rate from an upper edge site to a lower edge site and that from the lower edge site to a terrace site is just equal to the product of the hopping rates of the reverse processes. The observed difference[7] between step-up diffusion and step-down diffusion may be caused by the breaking of this relation. The surface electromigration[18] is considered as one of the origins of this difference.

In this paper, regular step array or periodic kink arrangement was assumed. It is interesting to study the step fluctuation effect on surface diffusion. Now its study is planned with use of the terrace-step-kink model[19,20] for a vicinal surface at finite temperature. Finally it is remarked that Eq. (13) gives the general relation between the hopping rates and the diffusion coefficient. So it is promising to apply Eq. (13) to the study of diffusion on reconstructed surfaces with superstructure. In these systems, plural unequivalent adsorption sites exist in a unit cell.

ACKNOWLEDGMENTS

One of the authors (A.N.) is grateful to Professor V. Heine for his continuing encouragement. She also expresses thanks to Dr. G. Rajagopal for his help with the computer system in the Cavendish Laboratory.

*Permanent address: The University of Electro-Communications, Chofu, Tokyo 182, Japan.

[1]P. M. Petroff, A. C. Gossard, and W. Wiegmann, Appl. Phys. Lett. **45**, 620 (1984).
[2]J. H. Neave, P. J. Dobson, B. A. Joyce, and J. Zhang, Appl. Phys. Lett. **47**, 100 (1985).
[3]C. A. Roulet, Surf. Sci. **36**, 295 (1973).
[4]R. Butz and H. Wagner, Surf. Sci. **87**, 85 (1979).
[5]E. Suliga and M. Henzler, J. Phys. C **16**, 1543 (1983).
[6]N. Wu, H. Yasunaga, and A. Natori, Surf. Sci. **260**, 1206 (1992).
[7]L. L. Levenson, H. Usui, I. Yamada, T. Takagi, and A. B. Swartzlander, J. Vac. Sci. Technol. A **7**, 1206 (1989).
[8]A. F. Voter, Proc. SPIE **821**, 214 (1987).
[9]C. Liu and J. B. Adams, Surf. Sci. **265**, 262 (1992).
[10]K. D. Hammonds and M. Lynden Bell, Surf. Sci. **278**, 437 (1992).
[11]K. Shiraishi, Appl. Phys. Lett. **60**, 1363 (1992).
[12]E. V. Albano, K. Binder, D. W. Heermann, and W. Paul, Surf. Sci. **223**, 151 (1989).
[13]R. L. Schwoebel, J. Appl. Phys. **37**, 3682 (1966).
[14]R. L. Schwoebel, J. Appl. Phys. **40**, 614 (1969).
[15]R. Gomer, Rep. Prog. Phys. **53**, 917 (1990).
[16]P. J. Reynolds and D. M. Ceperley, J. Chem. Phys. **77**, 5593 (1982).
[17]K. Binder and D. Staufer, in *Applications of Monte Carlo Method in Statistical Physics,* edited by K. Binder (Springer, Berlin, 1984), p. 1.
[18]H. Yasunaga and A. Natori, Surf. Sci. Rep. **15**, 205 (1992).
[19]W. Selke and A. M. Szpilka, Z. Phys. B **62**, 381 (1986).
[20]N. C. Barlet, T. L. Einstein, and E. D. Williams, Surf. Sci. **244**, 149 (1991).